Marching Through the Visible Man

Bill Lorensen
GE Corporate Research and Development

Abstract. The National Library of Medicine is creating a digital atlas of the human body. This project, called the Visible Human, has already produced computed tomography, magnetic resonance imaging and physical cross-sections of a human male cadaver. This paper describes a methodology and results for extracting surfaces from the Visible Male's CT data. We use surface connectivity and isosurface extraction techniques to create polygonal models of the skin, bone, muscle and bowels. Early experiments with the physical cross-sections are also reported.

1. Introduction

In 1989, the National Library of Medicine (NLM) began an ambitious project to create a digital atlas of the human anatomy. The NLM *Planning Panel on Electronic Image Libraries* [1] recommended a project to create XRAY Computed Tomography (XRAY-CT), Magnetic Resonance Imaging (MRI) and physical sections of a human cadaver. The project is called "The Visible Man." Another cadaver, that of a 59 year-old woman, is being processed and "The Visible Woman" should be completed in the Summer of 1995.

Our laboratory has a long history of constructing 3D models from contiguous CT and MRI cross-sections. The Visible Man data sets provide an opportunity to test our algorithms on publicly available data. The data is interesting because of its size and variety of modalities. Also, its availability on the Internet means that other researchers can apply their algorithms to a common data set. In the past it has been difficult to obtain medical data because of patient confidentiality.

This paper reports our early experiments with the Visible Man CT data in the hopes that others will benefit from our experiences. The paper proceeds as follows. First we briefly discuss the background on the "Visible Man" and the four data sets. We describe the logistics of working with such large data sets and summarize the various parameters for the fresh CT data. Then, we propose a methodology for reporting algorithm results. We describe the methods and materials we used to create the models illustrated in subsequent sections.

2. The Visible Man

In August of 1991 NLM awarded a contract to the University of Colorado Health Sciences Center to create the digital cross-sections of a 39-year old convicted murderer who had donated his body to science. The radiological data was created using commercial MRI and XRAY-CT. Two CT data sets were created: one of the fresh cadaver, the other after the cadaver was frozen. Then, the cadaver was embedded in gelatin, frozen and sliced from head to toe. As each layer was exposed, a color RGB photograph was taken. Over 1800 24-bit images 2048 by 1216 were created.

2.1 The Fresh CT Data Set

Since we have experience working with radiological cross-sections from CT and MRI, our initial experiments used the CT data. We chose the fresh CT data because there is better soft tissue contrast from the data taken before the subject was frozen. Also, the fresh CT data is

the most manageable of the four data sets. And, segmentation of soft tissue / air boundaries and bone are particularly easy for CT data. Compared to the MRI data, the slice spacing of the CT data is sufficient to produce decent 3D models.

2.2 Logistics

We obtained the fresh CT data using *ftp* via the Internet. Internet access is available to users that sign a license agreement with NLM. A summary of the project and information on how to obtain the data sets are available through the World Wide Web [2]. The data is stored one slice per file and the files have been compressed using the unix *compress* program. Uncompressed, each slice is 512 x 512 x 16 bits with a 3416 byte header. The format of the headers is General Electric Genesis described in the Medical Image Format FAQ [3]. The image header contains among other things the table position and field of view. These are important quantities when working with this data since the spacing between the slices and the pixel size changes several times throughout the data set. The slices are named as follows: c_vm*xxxx*.fre where *xxxx* is the location in mm's of the slice. There are 522 slices in the fresh CT data set using about 274 megabytes of disk storage.

2.3 Description of the CT data from headers

The first step to understand the data was to print the header information. In particular, we need to know the size of the pixels, and the distance between each slice. Also the order of acquisition is important so that we retain the proper left / right correspondence. In the fresh CT data set, the order of acquisition was from top to bottom.

The fresh CT data was acquired in several sections with varying pixel size and slice spacing. Because of this, we broke the data set into nine sections. We created a new section when at least one of three changes occurred in the slice headers:

1.Change in field of view (fov).
2.Change in slice spacing.
3.Gap in acquisition.

Table1 summarizes the data for the nine sections.

Section #	Slices	#	Fov	Pixel Size	Spacing	Aspect Ratio	Location
0	1-8	8	250	.488281	1	2.048	390-383
1	9-67	59	460	.8984375	1	1.11304	382-324
2	68-150	83	345	.673828	1	1.48406	323-241
3	151-191	41	450	.8789063	3	3.41333	240-120
4	192-246	55	460	.8984375	3	3.33913	117- -45
5	247-258	12	460	.8984375	3	3.33913	-51 - -84
6	259-418	160	460	.8984375	3	3.33913	-90 - -565
7	419-480	62	480	.9375	5	5.33333	520 - 215
8	481-522	42	480	.9375	5	5.33333	-210 - -415

TABLE 1. Section Definitions.

3. Define a Methodology

We propose a simple methodology to report results on the Visible Human data sets. These are by no means rigid rules, just guidelines for reporting results. The goal is to allow researchers to reproduce the results reported by others and to compare their results.

1. Define methods and materials. Identify the software used in each processing step and the origin of the software. Cite any references that describe the algorithms. Describe the hardware configurations used for processing the data.
2. Define parameters for each algorithm. Be specific enough so that another researcher, using the same or similar software, could reproduce the results. Parameters include region of interest coordinates, threshold values, opacity values and connectivity seeds.
3. Report results Include timings for each step. Although the actual times often depend on particular implementations, these times will give the reader a general feel for the processing times.

If additional images or animations are available report the site where they can be obtained. Use Uniform Resource Locators (URL's) when appropriate.

4. Our Methodology

4.1 Hardware

This work was done on an Onyx Reality Engine 2 (Silicon Graphics, Mountain View, CA) with the following configuration:

2 150 MHZ IP19 Processors
CPU: MIPS R4400 Processor Chip Revision: 5.0
FPU: MIPS R4010 Floating Point Chip Revision: 0.0
Data cache size: 16 Kbytes
Instruction cache size: 16 Kbytes
Secondary unified instruction/data cache size: 1 Mbyte
Main memory size: 256 Mbytes, 2-way interleaved

4.2 Software

The Reality Engine was running Irix 5.3. We used a variety of software tools we call the *Research Workstation* all developed in-house. All of the software works with 16-bit medical images.

Mrx is an image display package that allows users to access medical images stored in a variety of formats. We use it to inspect the image data and select thresholds for surfaces.

Surf3d is a surface tracking connectivity program [4] that takes user specified seed points and marks all voxels that are connected to the initial seeds and that satisfy a threshold range.

Softreformat is a volume reformatting program that uses tri-linear interpolation to resample volume data on arbitrary planes.

Cubes implements the *Marching Cubes* algorithm [5] and creates triangles from volume data. This implementation can process all of a volume, or only those voxels whose connectivity bit has been set by *surf3d*.

LYMB [6] is an object-oriented development system written in C that permits object creation and modification through a scripting language. The objects in *LYMB* are C modules that implement methods in C procedures. One of these objects, *decimate*, implements the triangle decimation algorithm described in [7]. We use *decimate* to reduce the number of triangles in the models created by *cubes*. *LYMB* also has extensive visualization and rendering capabilities. A user interface and rendering subsystem in *LYMB* were used to cre-

ate the images in the paper.

5. Results

We applied a single methodology to extract skin, bone, muscle, and the bowels from the fresh CT data. Figure1 shows the data flow for our surface extraction technique. The connectivity and decimation steps are optional.

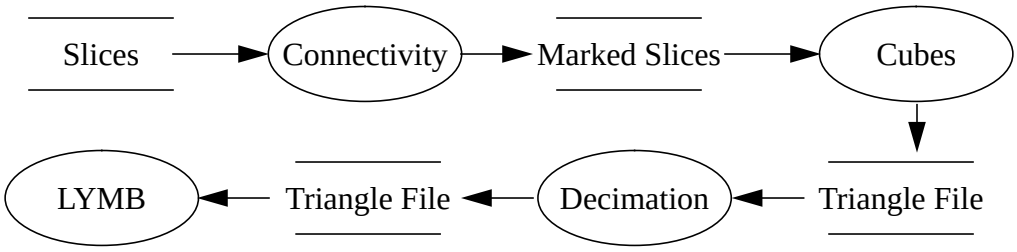

FIGURE 1. Data flow to create models.

5.1 Bone and Skin

We used the same threshold throughout the 9 sections of the CT data set to extract the skin and bone. For the skin, we applied the connectivity algorithm followed by Marching Cubes with a density value of 600 to remove the patient table and internal air passages from the extracted surfaces. We also applied two iterations of the decimation algorithm to the skin surface. We started with a decimation value of .0002 (or 2%) of the field of view. The skin has less detail than the internal surfaces and we can afford to reduce the number of skin triangles more heavily than for the internal surfaces. We did not apply connectivity for the bone surface since there are many disconnected pieces of bone in the body. A density value of 1224 was used for the bone, the same value we have used successfully on other CT data sets. Table 2 shows triangle counts and timings for the skin surfaces. Table 3 shows the tim-

Section	Connect(tri's)	Time(sec)	Cubes(tri's)	Time(sec)	Decimation(tri's)	Time(sec)
0	31616	0.67	63662	4.14	27168	14.24
1	65584	4.01	131448	18.17	53362	28.27
2	139922	6.20	281013	30.00	96354	68.54
3	115732	3.28	231683	18.52	77861	54.01
4	139624	4.38	277848	23.71	70773	82.61
5	27213	0.91	54476	4.76	12480	20.28
6	524253	14.04	1049476	79.69	295077	322.05
7	167288	5.07	334643	30.32	84342	89.46
8	93266	2.90	186630	17.08	71485	43.04
Totals	1304498	41.46	2610877	226.39	798227	722.50

TABLE 2. Triangle Counts and Times for Skin.

Section	Cubes (tri's)	Time(sec)	Decimation(tri's)	Time(sec)
0	38394	6.23	17799	7.64
1	257356	49.06	139852	47.31
2	865454	93.78	541654	135.41
3	193102	34.24	137717	28.63
4	915904	77.94	679246	125.05
5	158174	14.58	118091	20.90
6	1990946	199.20	1501322	273.11
7	74864	41.58	49610	12.46
8	220916	33.16	168579	28.39
Totals	4715110	549.77	3353870	678.9

TABLE 3. Triangle Counts and Times for Bone.

ings and counts for the bone. The times for each step are central processor unit (CPU) times. The images in Figure 2 where created using *LYMB*. The surfaces for each section were manually aligned using an interactive rendering interface in *LYMB*. We chose section 6 as the center of the model and moved the other sections relative to this surface. Table 4 shows the

Section	x	y	z
0	104	165	482
1	0	0	473
2	57	57	413
3	5	5	330
4	0	0	207
5	0	0	39
6	0	0	0
7	-13	-8	-480

TABLE 4. Offsets (in mm's) for each section.

relative movements of each section measured in millimeters.

We also reconstructed coronal cross-sections for each of the data sets using the *softreformat* program of the Research Workstation, composing the reformatted image in Figure 2 using Jeff Poskanzer's Portable Bitmap utilities [8]. The gaps in the reformatted images show the boundaries of the 8 sections (the 9th contains the feet and is not contiguous with the other sections).

5.2 Bowels.

The bowels, shown in Figure 3, were extracted from section 6 by first running the connectivity algorithm and then Marching Cubes with a density of 700. The muscle was similarly extracted using connectivity and Marching Cubes with a density of 1010. The region of interest for the muscle was restricted to slices 100 - 160 because the CT scan artifacts higher in the body caused the connectivity algorithm to leak. Two decimation iterations were applied to both the muscle and bowel surfaces. The bowels were colored with (red, green, blue) values of (.89, .81, .34) with a specular component of .4 and a specular power of 10. The muscle color is (.6980, .1333, .1333), specular component .4 and specular power 10. We created a separate back face property for these two surfaces by reducing the diffuse

component of each material to .4. This surface visualization technique is useful to give the viewer a clue as to which surface is an outward surface and which is an inward surface.

5.3 Muscles in the Leg.

The thigh muscles are in section 7. We extracted them using the same density value, 1010, that we used in section 6. A separate connectivity seed was specified for each muscle. Figure 4 shows the bone, muscle and transparent skin for the resulting surfaces.

5.4 Flying Through the Body.

We created a fly through the bone surfaces extracted for the whole data set. We first rendered the skin model for each section properly displaced. Then, using the picking facility in *LYMB*, we selected 40 points with a mouse from the skin to serve as key frames for an animation. We key framed both the camera *look from* and *look at* points using consecutive picked points. *LYMB* created a smooth camera motion by interpolating the *from* and *to* points using splines [9]. We specified 1 second of animation between each key frame point, resulting in 1200 animation frames. Before rendering the sequence, we turned off the skin surface, rendered each frame and saved them to disk. The Silicon Graphics *movieconvert* program created a lossless QuickTime movie. After transferring the 550 megabyte QuickTime movie to a Macintosh, we single frame recorded the animation using the DiaQuest *animaq* software controlling a JVC BR-S811U S-VHS VCR. Figures 5 and 6 shows two frames from the resulting animation.

5.5 Working with the Physical Cross-Sections.

We have done some preliminary investigation of the physical cross-sections. Here we split each color physical cross-section into its red, green and blue components shown in Figure 7. Then, we applied the grey-scale algorithms described above to the red channel only. Figure 8 shows two views of the extracted skin surface from 215 slices. We selected the outer skin by first running the connectivity program marking 1538827 voxels and then extracting 3106832 triangles in 181 seconds. We ran two decimation iterations that removed 1226351 triangles.

6. Conclusions

The National Library of Medicine through the Visible Human Project has provided the medical research and educational community with a rich set of anatomical data. The general availability of the data will encourage researchers to develope new algorithms and compare their work with others. Our experience with that data has been positive although any group working with the data must be prepared to dedicate large amounts of disk storage and computer resources to the project. Practically, most groups will work with subsets of the data, concentrating on perhaps a few anatomical parts of regions. We expect that the major effort in the next few years will be to segment the Visible Man (and Woman). Such a large task will require cooperation of many research groups throughout the world. Central repositories of segment information will be required and we hope the NLM will be able to provide such facilities.

7. Acknowledgments

Most of this work was performed while the author was a visiting scientist at the Center for In-Vivo Microscopy at Duke University Medical Center. Al Johnson, Director of the Labo-

ratory, and his staff provided a rich hardware and software environment for these experiments. Others will find that working with such large data sets puts pressure on most laboratory resources.

8. References

[1] National Library of Medicine (U.S.) Board of Regents. Electronic imaging: Report of the Board of Regents. U.S. Department of Health and Human Services, Public Health Service, National Institutes of Health, 1990. NIH Publication 90-2197.

[2] http://www.nlm.nih.gov/extramural_research.dir/visible_human.html

[3] http://www.rahul.net/dclunie/medical-image-faq/html

[4] Cline, H. E., Dumoulin, C. L., Lorensen, W. E., Hart, H. R., and Ludke, S., "3D Reconstruction of the Brain from Magnetic Resonance Images Using a Connectivity Algorithm," *Magnetic Resonance Imaging*, vol. 5, no. 5, pp. 345-352, 1987.

[5] Lorensen, W. E. and Cline, H. E., "Marching Cubes: A High Resolution 3D Surface Construction Algorithm," *Computer Graphics*, vol. 21, no. 3, pp. 163-169, July 1987.

[6] Schroeder, W., Lorensen, W., Montanaro, G. and Volpe, C., "Visage: An Object-Oriented Scientific Visualization System," in *Proceedings of Visualization '92*, IEEE Press, October 1992, pp. 219-226.

[7] Schroeder, W. J., Zarge, J., and Lorensen, W. E., "Decimation of Triangle Meshes," *Computer Graphics*, vol. 26, no. 2, pp. 65-70, August 1992.

[8] ftp://ftp.ee.lbl.gov:pbmplus*.tar.Z

[9] Kochanek, D. H. U. and Bartels, R. H., "Interpolating Splines with Local Tension, Continuity, and Bias Control," *Computer Graphics*, vol. 18, no. 3, pp. 33-41, July 1984.

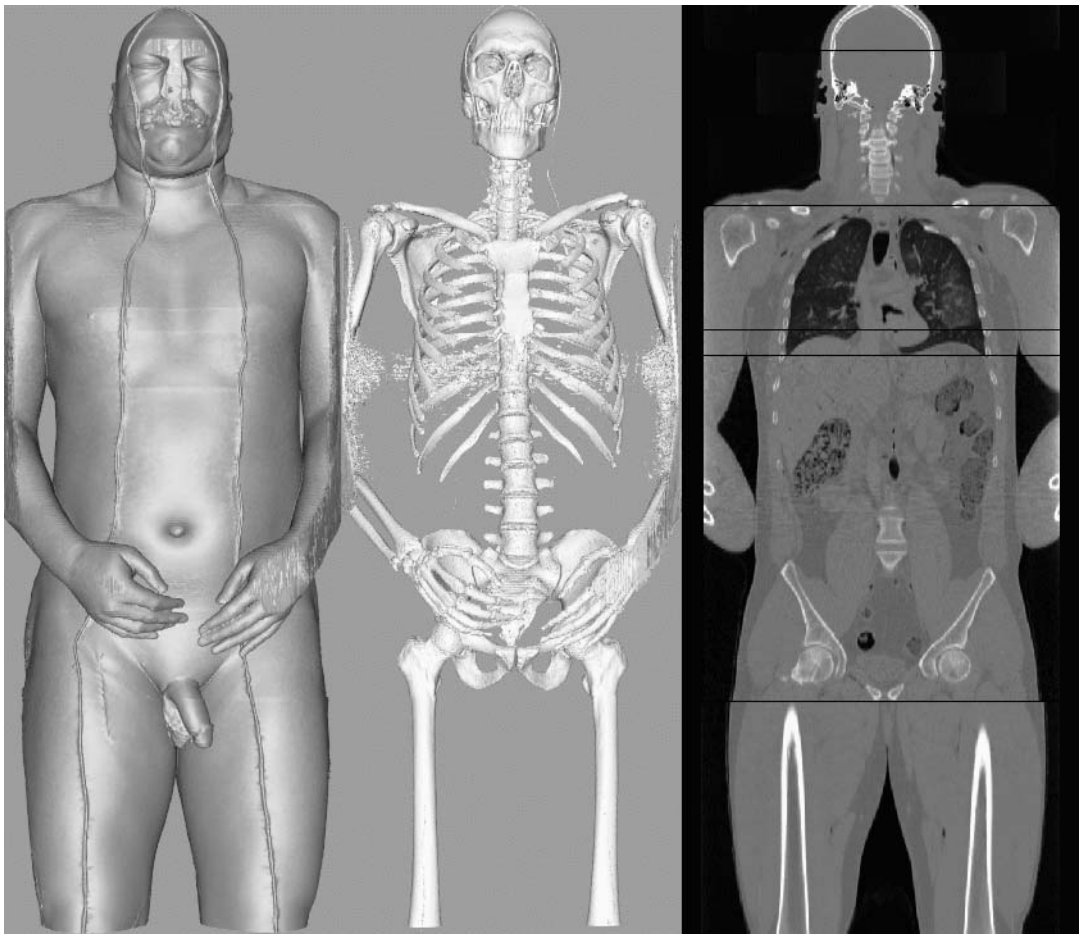

FIGURE 2. Skin, bone and reformatted Visible Man Fresh CT.

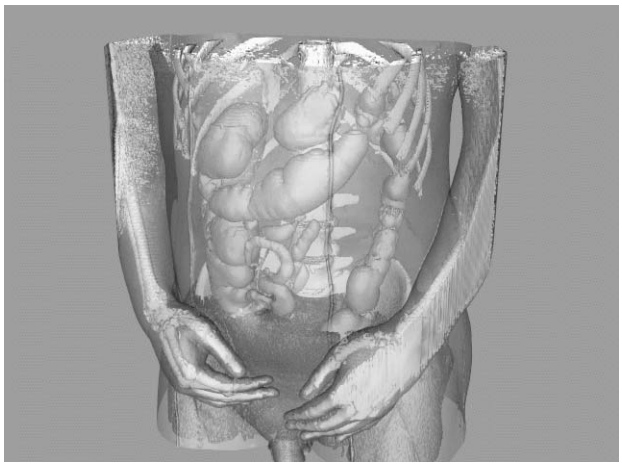

FIGURE 3. Bone, bowels, muscle and transparent skin from the abdomen.

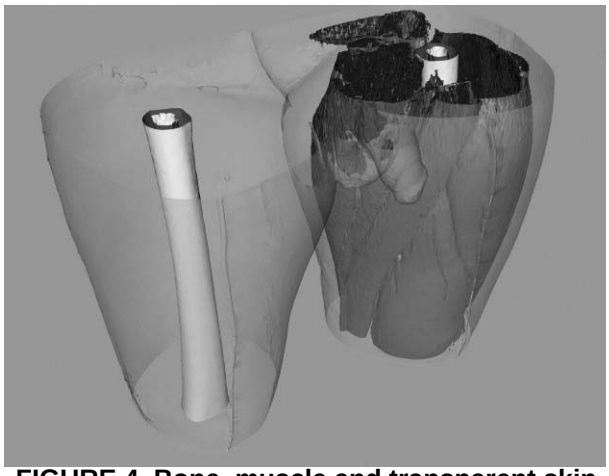

FIGURE 4. Bone, muscle and transparent skin from the thigh.

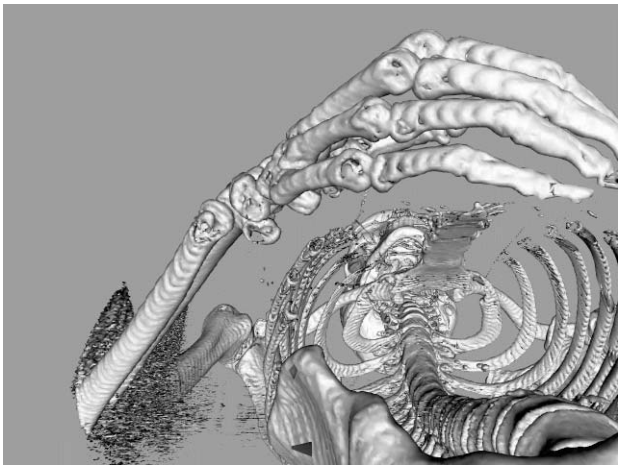

FIGURE 5. Flying up the Visible Man's thigh.

FIGURE 6. Flying up the Visible Man's spine.

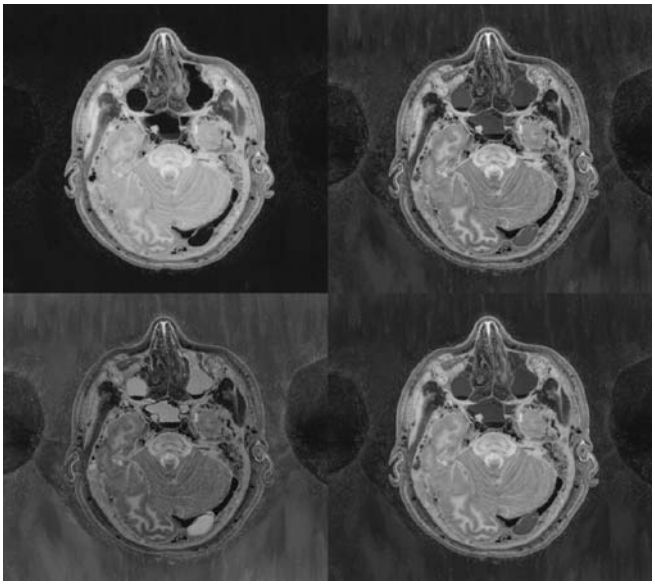

FIGURE 7. Red, green, blue and composite physical cross-section.

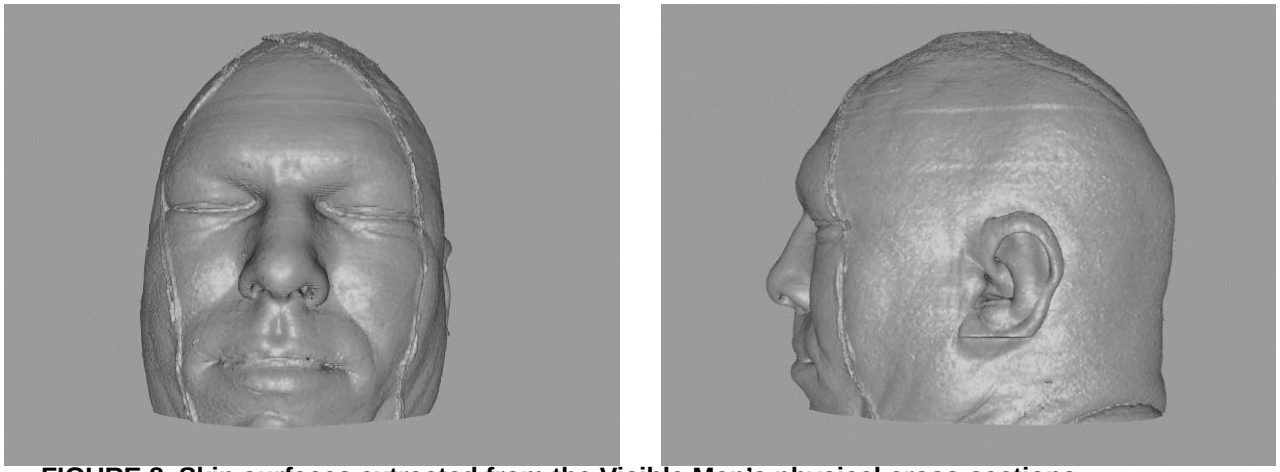

FIGURE 8. Skin surfaces extracted from the Visible Man's physical cross-sections.